

Medium modification of the pion-pion interaction at finite density

D. Davesne, Y. J. Zhang, and G. Chanfray

IPN Lyon, 43 Bd du 11 Novembre 1918, F-69622 Villeurbanne Cedex, France

(Received 4 April 2000; published 18 July 2000)

We discuss medium modifications of the unitarized pion-pion interaction in the nuclear medium. We incorporate both the effects of chiral symmetry restoration and the influence of collective nuclear pionic modes originating from the p -wave coupling of the pion to delta-hole configurations. We show in particular that the dropping of the sigma-meson mass significantly enhances the low-energy structure created by the in-medium collective pionic modes.

PACS number(s): 21.30.Fe, 21.65.+f

I. INTRODUCTION

Modifications of hadron properties in nuclear and hot hadronic matter is one of the central subjects of present day nuclear physics. For instance, it has been suggested in [1] that the in-medium pion-pion interaction might be significantly reshaped at density even below normal nuclear matter density. The basic mechanism is linked to the nuclear collective pionic modes, sometimes called pisobars, originating from the p -wave coupling of the pion to delta-holes states. According to detailed calculations [2,3] these collective modes are able to explain charge exchange data [4,5], despite the peripheral character of these experiments, although some other mechanisms such as broadening of the delta [6] or projectile excitation [7] have been proposed. In addition, other detailed studies show that collective effects are associated mainly with a particular channel such as the coherent pion one [8]. This medium effect yields a softening of the pion dispersion relation and consequently a modification of the two-pion propagator involved in the unitarized T matrix describing the pion-pion interaction at finite density. Indeed, on the basis of purely phenomenological models [9], an important reshaping of the pion-pion interaction in the scalar-isoscalar channel (sigma channel), producing a sizable accumulation of strength near the two-pion threshold, has been predicted. This problem has been reinvestigated with chiral symmetric models such as linear or nonlinear sigma models [10] with special emphasis on the consistency between chiral symmetry constraints and unitarization. It was soon realized that this medium effect is of considerable importance for the still open problem of nuclear saturation since an important part of the nucleon-nucleon interaction comes from correlated two-pion exchange and several papers have brought extremely interesting results [11–13]. Possible evidence for this reshaping of the π - π strength function is provided by the π - 2π data obtained on various nuclei by the CHAOS Collaboration at TRIUMF [14]. Recent calculations show that the observed marked structure in the $\pi^+\pi^-$ invariant mass spectrum can be partially explained by this reshaping [15,16]. These last results have been questioned in a recent paper [17] where it is found that pion absorption forces the reaction to occur at lower peripheral density.

However, what was ignored in the previous approaches was the possible medium modification of the basic π - π interaction, i.e. the π - π potential from the underlying quark

substructure or, in other words, from the in-medium modification of hadronic properties associated with chiral symmetry restoration. This may have considerable consequences since applying by hand in the linear sigma model pion-pion potential a Brown-Rho scaling of the sigma mass yields a significant enhancement of the near-threshold structure in the 2π strength function [18]. To go further, it is important to construct an in-medium π - π pion-pion potential. This question has already been addressed [19] in the framework of the Nambu–Jona-Lasinio (NJL) model at finite temperature. In this paper we will first use exactly the same scheme but with a straightforward generalization at finite constituent quark density to be identified later with one-third of the baryonic (i.e., nucleonic) density. In particular we will show that, using a slightly different prescription for the loop integrals, the NJL model regenerates the linear sigma model pion-pion Born term amplitude. This result, which is numerically extremely close to the more involved calculational scheme of Ref. [19], can be generalized at finite density and/or temperature provided the values of the pion mass, the sigma mass, and the pion decay constant are replaced by their in-medium values calculated in the NJL model. Using this scheme we are in position to study in a particularly simple way direct observable consequences of both partial chiral symmetry restoration such as the dropping of the sigma meson mass and collective p -wave pionic modes by looking at the in-medium pion-pion interaction in the scalar-isoscalar channel. This is of utmost importance since, as emphasized recently by Hatsuda *et al.*, the evolution of collective scalar-isoscalar modes, i.e., the sigma meson, may reveal precursor effects associated to chiral symmetry restoration [20].

From this density dependent effective linear sigma model potential implemented with a phenomenological form factor, it is possible to construct a unitarized π - π scalar-isoscalar amplitude which both preserves chiral symmetry constraints (Weinberg scattering length in the chiral limit) and reproduces experimental phase shifts. On top of precursor effects of chiral symmetry restoration, the inclusion of medium effects associated with the modification of the pion dispersion relation should be consistently done in the framework of the NJL model by direct coupling to constituent quarks populating the Fermi sea. However, the resulting pion p -wave polarizability calculated with quark-particles–quark-holes would completely miss the phenomenologically well established strong screening effects from short-range correlations

TABLE I. Physical quantities at $\rho=0$ in the NJL model for different parameters (I and II) and different schemes of calculations (exact and simplified).

	f_π (MeV)	m_π (MeV)	m_σ (MeV)	Λ (MeV)	m (MeV)	m_0 (MeV)	g (fm ²)
I (exact)	93.0	139.0	700.0	620.84	347.49	5.677	0.2247
II (exact)	93.0	139.0	1000.0	573.31	498.85	5.772	0.3303
I (simplified)	93.0	139.0	700.0	624.25	343.03	5.540	0.2207
II (simplified)	93.0	139.0	1000.0	573.60	495.15	5.712	0.3284

(g' parameter). Incorporation of correlation effects in the NJL model obviously requires a much more involved level of sophistication, hence losing the simplicity which is one of its main interests. Furthermore, we will calculate the in-medium two-pion propagator from standard pion-nucleus phenomenology. In other words, the p -wave pion polarizability will be taken as its nuclear matter expression dominated in the region of interest by the Δ -hole piece corrected by screening effects. The underlying philosophy can be summarized by saying that the medium modified soft physics linked to chiral symmetry (m_π, f_π , low-energy π - π potential) is calculated within the NJL model while p -wave physics yielding pionic nuclear collective modes is described through standard nuclear phenomenology.

II. π - π INTERACTION FROM THE NJL MODEL

To examine the π - π interaction at finite density (and finite temperature), we start from the SU(2) version of the well-known NJL model [21]:

$$\mathcal{L} = \bar{\psi}(i\partial - m_0)\psi + g[(\bar{\psi}\psi)^2 + (\bar{\psi}i\gamma_5\tau\psi)^2], \quad (1)$$

where g is a coupling strength of dimension [mass]⁻², and m_0 is the current quark mass. To maintain the asymptotic freedom at high energies, we simulate the situation by regarding the coupling constant in Eq. (1) as a momentum dependent one, $g(p)$:

$$g(p) = g \prod_{i=1}^4 \theta(\Lambda - |\mathbf{p}_i|), \quad (2)$$

where \mathbf{p}_i 's are the momenta of quarks and θ is the step function. Three parameters, namely, g , Λ , and m_0 , are determined to reproduce the pion mass m_π , the pion decay constant f_π , and the mass of the sigma meson m_σ . Here for m_π and f_π we choose the well-accepted values, and for m_σ we select two different empirical values to test the influence of the input data on our final results. In Table I, we list two sets of values for m_π , f_π , and m_σ , and also g , Λ , and m_0 which are fixed, respectively, to give these two sets of values of m_π , f_π , and m_σ . In the parameter fitting, we follow the formalism in the paper of Hatsuda, and Kunihiro [22], where the three-momentum cutoff was used. With the lowest value of $m_\sigma=700$ MeV, one has a set of parameters very close to the one of Quack *et al.* [19] used for finite temperature studies. In the following mainly devoted to finite density, we will prefer the second set with $m_\sigma=1$ GeV for two reasons. On

the one hand, this second set gives a higher density for chiral symmetry restoration (about $2.6\rho_0$ in place of $1.5\rho_0$), and on the other hand, the values of $m_\sigma=1$ GeV has been successfully used in previous works to fit the vacuum π - π data [10,15].

In Table I, we also include the results with different schemes of calculation, the ‘‘exact’’ one and the ‘‘simplified’’ one. For the ‘‘exact’’ scheme, we just do the same calculation as Quack *et al.* [19] but at finite density, while for the ‘‘simplified’’ one, we neglect the q^2 dependence in all of the integrals (for details see Sec. III) in our calculation, where q is the external momentum of pion and sigma mesons.

The main purpose of this section is to get the density dependence on the π - π scattering length a^I , which is related to the π - π scattering amplitude T^I at threshold as

$$a^I = -\frac{1}{32\pi m_\pi} \text{Re} T^I, \quad (3)$$

where I is the total isospin.

To the lowest order in $1/N_c$ (N_c , the number of quark colors), the invariant amplitude $\mathcal{T}_{ab;cd}$ of the π - π scattering process (a, b and c, d are the isospin indices) is calculated from the box and σ -propagation diagrams shown in Fig. 1 (see Fig. 1 in Ref. [19]). Following the notation of Ref. [19], we have

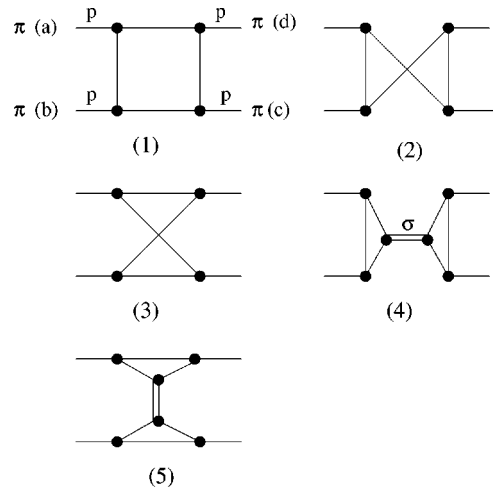


FIG. 1. Box and σ -propagation diagrams for π - π scattering (a),(b),(c), and (d) are the isospin indices.

$$\begin{aligned} \mathcal{T}_{ab;cd} = \langle cp_c ; dp_d | \mathcal{T} | ap_a ; bp_b \rangle = & A(s,t,u) \delta_{ab} \delta_{cd} \\ & + B(s,t,u) \delta_{ac} \delta_{bd} + C(s,t,u) \delta_{ad} \delta_{bc}, \end{aligned} \quad (4)$$

$$\mathcal{T}^2 = 2\mathcal{T}_3 + 2\mathcal{T}_5, \quad (10)$$

where s , t , and u are the usual Mandelstam variables: $s = (p_a + p_b)^2$, $t = (p_a - p_c)^2$, and $u = (p_a - p_d)^2$.

Because of the crossing relations, there are three possibilities for the box diagram [23] which, after a direct evaluation, gives

$$\begin{aligned} (\mathcal{T}_1)_{ab;cd} = & -(\delta_{ab}\delta_{cd} + \delta_{ac}\delta_{bd} - \delta_{ad}\delta_{bc}) [4N_c N_f i g_{\pi qq}^4] \\ & \times [I(0) + I(p) - p^2 K(p)], \\ (\mathcal{T}_2)_{ab;cd} = & -(\delta_{ab}\delta_{cd} - \delta_{ac}\delta_{bd} + \delta_{ad}\delta_{bc}) [4N_c N_f i g_{\pi qq}^4] \\ & \times [I(0) + I(p) - p^2 K(p)], \\ (\mathcal{T}_3)_{ab;cd} = & -(-\delta_{ab}\delta_{cd} + \delta_{ac}\delta_{bd} + \delta_{ad}\delta_{bc}) [8N_c N_f i g_{\pi qq}^4] \\ & \times [I(0) + p^4 L(p)/2 - 2p^2 K(p)], \end{aligned} \quad (5)$$

in terms of integrals $I(0)$, $I(p)$, $K(p)$, and $L(p)$ (see the Appendix).

The diagram with intermediate σ propagation shown in Fig. 1 can be simply expressed in terms of its components. By combination, one has

$$\begin{aligned} (\mathcal{T}_4)_{ab;cd} = & -\delta_{ab}\delta_{cd} g_{\pi qq}^4 [\Gamma^{\sigma\pi\pi}(p, -p)]^2 D_\sigma(2p), \\ (\mathcal{T}_5)_{ab;cd} = & -(\delta_{ac}\delta_{bd} + \delta_{ad}\delta_{bc}) g_{\pi qq}^4 [\Gamma^{\sigma\pi\pi}(p, p)]^2 D_\sigma(0), \end{aligned} \quad (6)$$

where

$$\begin{aligned} \Gamma^{\sigma\pi\pi}(p, -p) = & -8N_c N_f m I(p), \\ \Gamma^{\sigma\pi\pi}(p, p) = & -8N_c N_f m [I(0) - p^2 K(p)] \end{aligned} \quad (7)$$

are the σ - π - π vertex in the s channel and t channel, respectively, and

$$D_\sigma(k) = \frac{i}{2N_c N_f [(k^2 - 4m^2)I(k) - m_\pi^2 I(m_\pi)]} \quad (8)$$

is the sigma meson propagator. Similar to Eq. (8), we also have [19,23]

$$g_{\pi qq}^{-4} = -N^2 [I(0) + I(p) - m_\pi^2 K(p)]^2 \quad \text{with } N = N_c N_f. \quad (9)$$

We note here that all above results are evaluated at threshold ($p_i^2 = p^2 = m_\pi^2 = s/4$), and we restrict them, for $T > 0$, to the scattering of pions whose c.m. system is at rest in the heat bath [19].

Summing Eqs. (5) and (6) and with the help of projection of the amplitudes on total isospin I , one finds the s -wave scattering amplitudes

$$\begin{aligned} \mathcal{T}^0 = & 6\mathcal{T}_1 - \mathcal{T}_3 + 3\mathcal{T}_4 + 2\mathcal{T}_5 \\ \mathcal{T}^1 = & 0, \end{aligned}$$

where the \mathcal{T}_i are the function in Eqs. (5) and (6) expected of the isospin factors. To get the density dependence on \mathcal{T}_i , we must calculate the constituent quark mass m and the pion mass m_π at finite density first.

As in Ref. [22], we get the in-medium constituent quark mass from the gap equation due to the one-loop quark self-energy diagram (Fig. 5 in Ref. [22]). The in-medium pion mass (and also σ -meson mass) is determined from the dispersion relation (in the $\mathbf{q} \rightarrow \mathbf{0}$ limit) of the meson excitation (which itself is the solution of the Dyson equation in the ring-diagram approximation). For the details of deriving the gap equation for quarks and the dispersion relation for π (and also σ) meson, one can resort to Refs. [19,22] with a straightforward extension at finite density. Some specific results and integrals are explicitly given in the Appendix. Here we display only the final results evolving with respect to density at zero temperature. One thing to be mentioned here is that there are two different definitions for the coupling between pions and quarks, namely, $g_{\pi qq}$: one is from Hatsuda and Kunihiro [22] and the other is from Quack *et al.* [19]. These two $g_{\pi qq}$ differ from each other only by a term proportional to

$$\beta \int dk \frac{k^2}{E^2} f(E) f(-E) F(E, p),$$

where β is the inverse of the temperature, $f(E)$ the Fermi-distribution function, and $F(E, p)$ a rational fraction of E ($E = \sqrt{m^2 + \mathbf{k}^2}$) and p (external momentum of pions). It turns out that this term disappears when the temperature goes to zero. So the discrepancy between these two definitions will not give rise to any difference in the parameter fitting which is done only at zero temperature and also in the main part of this paper as we focus our calculation on the cases of finite density but at zero temperature.

The density dependence of constituent quark mass, π mass, σ mass, and f_π is shown in Fig. 2. We find that all these quantities evolve with density almost linearly except in the high density region (say $\rho > 0.30 \text{ fm}^{-3}$) and the trends of these curves are all the same as those evolving with temperature [22]. Here we use two sets of parameters listed in Table I.

We first show that the density dependences of the threshold amplitudes and scattering lengths are very similar to those obtained at finite temperature in [19]. In Fig. 3, we draw the curves of the various pieces of the scattering amplitudes as a function of density (at zero temperature) with both sets of parameters. Again, we see that all the curves evolve linearly with density in the low- and medium-density region. At a certain density ρ_d , there exists a divergence as at high temperature [19]. Similar behavior also holds in Fig. 4 where the relation between scattering length and density is illustrated. An interesting feature is that one gets a higher value of density ρ_d with the higher input vacuum σ -meson mass. This divergence occurring in the sigma propagator [19] actually corresponds to the point where the in-medium

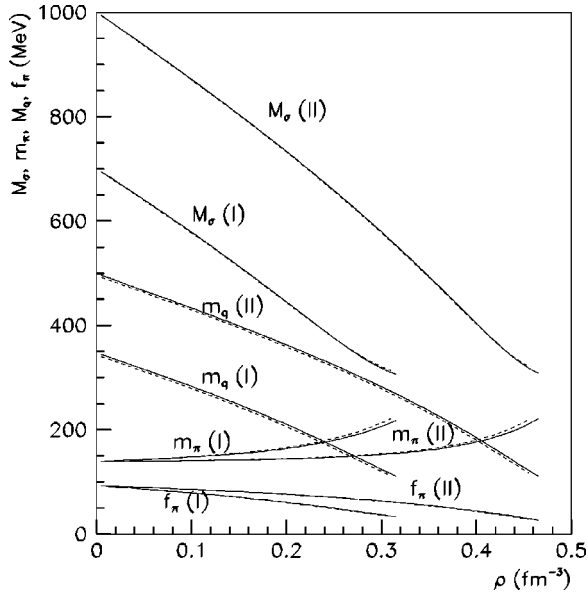


FIG. 2. Constituent quark mass m , pion mass m_π , σ -meson mass m_σ , and pion decay constant f_π vs density (at zero temperature) with parameter sets I and II: solid lines for the exact calculation and dashed lines for the simplified calculation.

sigma mass drops to twice the in-medium pion mass. In the second set of parameters the density ρ_d turns out to be $\rho_d \sim 2.4\rho_0$. Once unitarization is done (see Sec. V) this density goes down to about $\rho_d \sim 2\rho_0$ due to the presence of the two-pion loop in the sigma propagator. We will come to this important point in Sec. V since, as pointed out by Hatsuda *et al.* [20], the vanishing of the real part of the inverse sigma propagator at $E=2m_\pi$ can be seen as a precursor effect of chiral symmetry restoration. However, the aim of this paper is not primarily to study the phase transition region but the

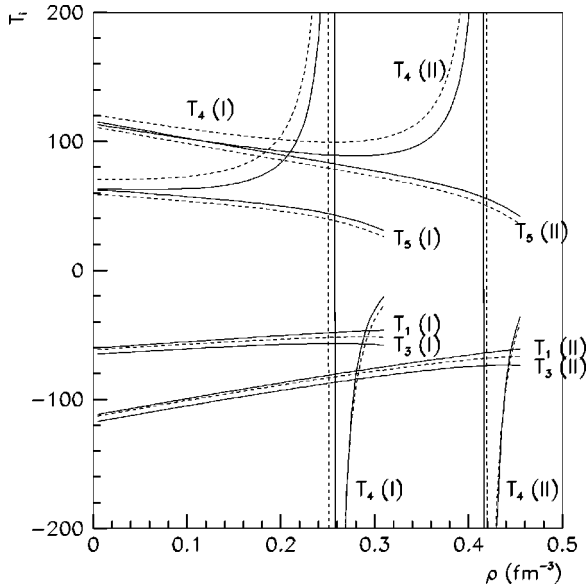


FIG. 3. Scattering amplitudes T_i vs density (at zero temperature) with parameter sets I and II: solid lines for the exact calculation and dashed lines for the simplified calculation.

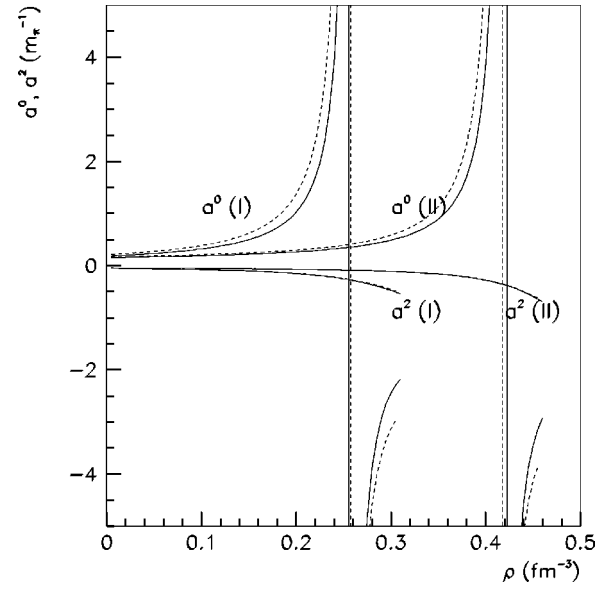


FIG. 4. Scattering lengths a^0 and a^2 vs density (at zero temperature) with parameter sets I and II: solid lines for the exact calculation and dashed lines for the simplified calculation.

moderate density region below nuclear matter density accessible in the π - 2π experiment. For that purpose, we show in Fig. 5 the low density behavior of the scattering lengths.

III. SIMPLIFIED SCHEME

Now we turn to the simplified scheme of our calculation, where we neglect the momentum dependence in all of above integrals, i.e., $I(p)$, $K(p)$, and $L(p)$ (we will state later in this section the reason for such a treatment). But before this simplified processing, we would like to check whether the Weinberg limit is still kept at finite density and finite temperature. First we want to see how these integrals (and then other related quantities) behave in the first order chiral ex-

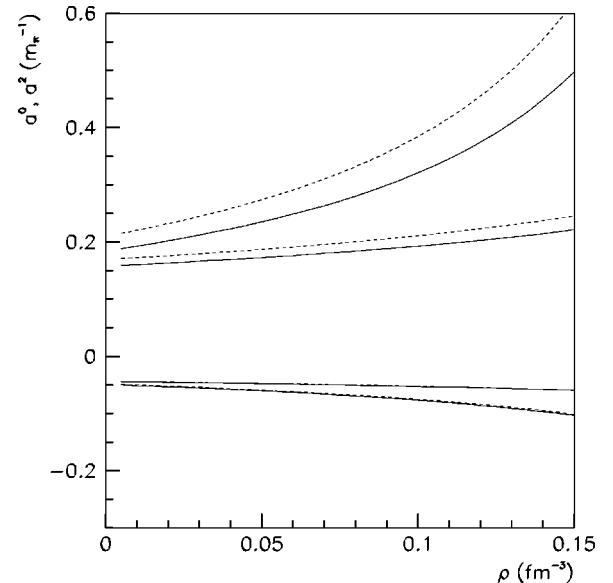


FIG. 5. Same as Fig. 4 but for a moderate range of density.

pansion (expanding to the order of m_π^2). Keeping in mind that we are always in the three-dimensional cutoff constraint and following the regularization of Ref. [23], we find after straightforward calculation that

$$I(p^2=m_\pi^2)=I(0)-\frac{1}{3}m_\pi^2K(0),$$

$$K(p^2=m_\pi^2)=K(0)-\frac{1}{2}m_\pi^2L(0),$$

$$L(p^2=m_\pi^2)=L(0)-\frac{5}{6}m_\pi^2I_{32}(0), \quad (11)$$

where $I_{32}(0)$ is shown explicitly in the Appendix. With these expansions, we get, from Eqs. (5)–(9),

$$\begin{aligned} \mathcal{T}_1 &= \frac{4i}{N\left\{2I(0)-\frac{1}{3}m_\pi^2K(0)-m_\pi^2\left[K(0)-\frac{1}{2}m_\pi^2L(0)\right]\right\}}, \\ \mathcal{T}_2 &= \mathcal{T}_1, \\ \mathcal{T}_3 &= \frac{8i\left\{I(0)+m_\pi^4\left[L(0)-\frac{5}{6}m_\pi^2I_{32}(0)\right]/2-2m_\pi^2\left[K(0)-\frac{1}{3}m_\pi^2L(0)\right]\right\}}{N\left\{2I(0)-\frac{1}{3}m_\pi^2K(0)-m_\pi^2\left[K(0)-\frac{1}{2}m_\pi^2L(0)\right]\right\}}, \\ \mathcal{T}_4 &= \frac{\left\{-8m\left[I(0)-\frac{1}{3}m_\pi^2K(0)\right]\right\}^2}{\left\{2I(0)-\frac{1}{3}m_\pi^2K(0)-m_\pi^2\left[K(0)-\frac{1}{2}m_\pi^2L(0)\right]\right\}^2} \frac{i}{2N\left\{(4m_\pi^2-4m^2)\left[I(0)-\frac{4}{3}m_\pi^2K(0)\right]-m_\pi^2\left[I(0)-\frac{1}{3}m_\pi^2K(0)\right]\right\}}, \\ \mathcal{T}_5 &= \frac{\left\{-8m\left[I(0)-m_\pi^2\left[K(0)-\frac{1}{3}m_\pi^2L(0)\right]\right]\right\}^2}{\left\{2I(0)-\frac{1}{3}m_\pi^2K(0)-m_\pi^2\left[K(0)-\frac{1}{2}m_\pi^2L(0)\right]\right\}^2} \frac{i}{2N\left\{-4m^2I(0)-m_\pi^2\left[I(0)-\frac{1}{3}m_\pi^2K(0)\right]\right\}}. \end{aligned} \quad (12)$$

Keeping to the first order of m_π^2 with the help of Eqs. (3) and (10), one finds finally that

$$a^0 = \frac{1}{32\pi m_\pi} \frac{7m_\pi^2}{f_\pi^2},$$

$$a^2 = \frac{1}{32\pi m_\pi} \frac{-2m_\pi^2}{f_\pi^2}, \quad (13)$$

where f_π is defined as in Ref. [22]. Note there that the functions $I(0)$, $K(0)$, $L(0)$, and $I_{32}(0)$ are the integrals at finite density and finite temperature. We thus recover the Weinberg limit (in the first order chiral expansion) at threshold for finite density and finite temperature.

In the simplified calculation, we neglect the momentum dependence of all above integrals inside the formula for \mathcal{T}_i , i.e., $p^2=m_\pi^2=0$, except that we keep k^2 in Eq. (8) unchanged as the momentum transfer in the two-pion interaction. Thus one gets

$$\mathcal{T}_1 = \mathcal{T}_2 = \mathcal{T}_3 = \frac{2i}{NI(0)},$$

$$\mathcal{T}_4 = \mathcal{T}_5 = \frac{8im^2}{NI(0)} \frac{1}{k^2 - m_\sigma^2}, \quad (14)$$

where $m_\sigma^2 = 4m^2 + m_\pi^2$ in the simplified calculation, which can be easily verified from Ref. [22]. Since $f_\pi^2 = -2iNm^2I(0)$ in the simplified calculation, the above amplitudes can be rewritten as

$$\mathcal{T}_1 = \mathcal{T}_2 = \mathcal{T}_3 = \frac{2i}{NI(0)} = -2\lambda,$$

$$\mathcal{T}_4 = \mathcal{T}_5 = 4\lambda^2 f_\pi^2 \frac{1}{k^2 - m_\sigma^2}, \quad (15)$$

with the $\sigma\pi\pi$ coupling constant λ defined by $2\lambda f_\pi^2 = m_\sigma^2 - m_\pi^2$ as in the linear sigma model (see, for instance, Sec. 4 of [10]). In other words, this simplified scheme yields ex-

actly the amplitudes of the linear sigma model but with λ , f_π , m_σ , and m_π being functions of density (and temperature). The numerical results for the simplified calculation are also displayed in Figs. 2–4 by dashed lines. We find that these two calculations have not much difference from each other except for the high-density region. So the simplified calculation is a rather good approximation to address in our region of interest the density dependence of m , m_π , m_σ , f_π , and even the scattering amplitude and scattering length.

IV. IN-MEDIUM UNITARIZED T MATRIX

We now incorporate the previous π - π amplitudes considered as a irreducible potential into a Lippman-Schwinger (LS) equation to get the unitarized T matrix in the scalar-isoscalar channel. However, when solving the LS integral equation, the use of the ‘‘exact’’ scheme with its full momentum dependence turns out to be of hopeless complexity. For this reason we prefer to use the potential from the ‘‘simplified scheme’’ which has been shown to be very close to the observables (pion decay constant, masses, scattering lengths) and their density dependences calculated with the ‘‘exact’’ scheme. Hence, the potential will be simply the linear sigma potential. For simplicity we restrict ourselves to an interacting pion pair with zero total momentum. In the scalar-isoscalar channel, the potential reads, with the obvious notations,

$$\begin{aligned} \langle \mathbf{k}, -\mathbf{k} | V(E) | \mathbf{k}', -\mathbf{k}' \rangle &= v(k)v(k') \frac{m_\sigma^2 - m_\pi^2}{f_\pi^2} \\ &\times \left(3 \frac{s - m_\pi^2}{s - m_\sigma^2} + \frac{t - m_\pi^2}{t - m_\sigma^2} + \frac{u - m_\pi^2}{u - m_\sigma^2} \right). \end{aligned} \quad (16)$$

The prescription for the Mandelstam variables to be used in the LS equation are the ones used in Sec. 4 of [10]. $E = \sqrt{s}$ is the energy variable at which the unitarized T matrix is calculated. t and u are chosen according to their on-shell values:

$$t = 2m_\pi^2 - 2\omega_k\omega_{k'} + 2\mathbf{k} \cdot \mathbf{k}', \quad u = 2m_\pi^2 - 2\omega_k\omega_{k'} - 2\mathbf{k} \cdot \mathbf{k}'. \quad (17)$$

The form factor $v(k)$, which is assumed to simulate the momentum dependence of the vertices, is to be fitted on experimental phase shifts and scattering lengths in the free case. The unitarized T matrix is the solution of the LS equation:

$$\begin{aligned} \langle \mathbf{k}, -\mathbf{k} | T(E) | \mathbf{k}', -\mathbf{k}' \rangle &= \langle \mathbf{k}, -\mathbf{k} | V(E) | \mathbf{k}', -\mathbf{k}' \rangle \\ &+ \frac{1}{2} \int \frac{d^3\mathbf{q}}{(2\pi)^3} \langle \mathbf{k}, -\mathbf{k} | V | \mathbf{q}, -\mathbf{q} \rangle \\ &\times G_{2\pi}(E, \mathbf{q}) \langle \mathbf{q}, -\mathbf{q} | V | \mathbf{k}', -\mathbf{k}' \rangle, \end{aligned} \quad (18)$$

where the two-pion propagator in vacuum is [10]

$$G_{2\pi}(E, \mathbf{q}) = \frac{1}{\omega_q} \frac{1}{E^2 - 4\omega_q^2 + i\eta}. \quad (19)$$

Ignoring the t and u dependence in the denominators, the potential [Eq. (16)] reduces to a combination of separable potentials. Taking parameter set II ($m_\sigma = 1$ GeV) implemented with a one-parameter form factor $v(k) = 1/(1 + k^2/64m_\pi^2)$, one exactly recovers the potential used in [10]. The phase shifts are correctly reproduced up to 800 MeV and the scattering length, $a_0 = 0.23m_\pi^{-1}$, is also in agreement with experimental data. It can be checked that, with such a separable potential, the correction to the scattering length from the unitarization procedure is of higher order in m_π^2 , thus preserving the chiral symmetry result (Weinberg scattering length) in the chiral limit.

From the underlying NJL quark model, the above results for the T matrix, Eqs. (16)–(19), can be generalized at finite density by simply replacing the pion mass, the sigma mass, and the pion decay constant by their in-medium values. With parameter set II, the pion mass does not change very much. Starting from the vacuum value $m_\pi = 139$ MeV, one finds at half nuclear matter density $m_\pi(\rho_0/2) = 140.3$ MeV and at saturation density $m_\pi(\rho_0) = 143$ MeV. The variation of the pion mass is usually expressed in terms of the s -wave pion optical potential or in term of an effective scattering length $\Delta m_\pi^2 = 2m_\pi V_{opt} = -4\pi(b_0)_{eff}\rho$. Here we find $(b_0)_{eff} \approx -0.01 m_\pi^{-1}$ which coincides with the experimental pion-nucleon scattering length. In reality the pion optical potential is more repulsive due to higher order rescattering effects but still giving a very small modification of the pion mass. Hence, this modification of the pion mass, which simulates s -wave pion-nucleus interaction, is practically negligible. In other words, the model does not give an unrealistically large shift in the pion mass.

On the contrary, there is a sizable dropping of the sigma mass of 110 MeV at half nuclear matter density and 225 MeV at normal density. Consequently, one finds a significant reshaping of the π - π strength function, as we will see in the next section, even at $\rho = 0.5\rho_0$ which is the typical density reached in π - 2π experiment [16]. We now come to study the dressing of the pion propagator by its p -wave coupling in matter. As already stated in the Introduction, the direct use of the standard NJL model for this problem would give totally unrealistic results since there is no repulsion and short-range correlation (g' parameter). Hence, we turn to a conventional nuclear matter description of the p -wave self-interaction of the pion on top of the NJL approach for the basic pion-pion potential. The pion propagator has the form

$$D_\pi(\mathbf{k}, \omega) = [\omega^2 - m_\pi^2 - \mathbf{k}^2 - S_\pi(\mathbf{k}, \omega)]^{-1}, \quad (20)$$

where $S_\pi(\mathbf{k}, \omega)$ is the conventional nuclear matter p -wave pion self-energy to be specified below. Notice that m_π is the in-medium pion mass calculated in the NJL model. According to the previous discussion, the small s -wave pion self-energy is partially accounted for but this gives in practice a negligible effect for the in-medium π - π T matrix. For this

first work, mixing the effects from the underlying quark structure (modification of $m_{\sigma,\pi}, f_\pi$) with those from pion p -wave coupling, we use the simplest possible approach. Hence, in the spirit of Ref. [9], we assume that the pion self-energy is dominated by virtual Δ - h excitations in the domain of energy of interest, namely,

$$S_\pi(\mathbf{k}, \omega) = k^2 \tilde{\Pi}^0(\mathbf{k}, \omega) = k^2 \Pi^0(\mathbf{k}, \omega) / [1 - g'_{\Delta\Delta} \Pi^0(\mathbf{k}, \omega)]. \quad (21)$$

Here $g'_{\Delta\Delta} \approx 0.5$ accounts for the short-range screening of the Δ - h polarization bubble Π^0 . The numerical calculations are performed in the framework of the two-level model already used in Ref. [9]. The main approximation of this model is to neglect the Fermi motion of the nucleons in the Δ - h bubble. In addition we first neglect the width of the delta resonance. This last approximation will be relaxed below. The polarization bubble has the form

$$\Pi^0(\mathbf{k}, \omega) = \frac{4}{9} \left(\frac{f_{\pi N\Delta}^*}{m_\pi} \Gamma(k) \right)^2 \rho \left(\frac{1}{\omega - \epsilon_{\Delta k} + i\eta} - \frac{1}{\omega + \epsilon_{\Delta k}} \right), \quad (22)$$

with $\epsilon_{\Delta k} = \sqrt{k^2 + M_\Delta^2} - M_N$ and $\Gamma(k)$ is the πNN form factor. It is a simple matter to show that the pion propagator takes the very simple form typical of a two-level model:

$$D_\pi(\mathbf{k}, \omega; \rho) = \frac{Z_1(k, \omega; \rho)}{\omega^2 - \Omega_1^2(k, \omega; \rho) + i\eta} + \frac{Z_2(k, \omega; \rho)}{\omega^2 - \Omega_2^2(k, \omega; \rho) + i\eta}, \quad (23)$$

where the eigenenergies Ω_1, Ω_2 and the strength factors Z_1, Z_2 ($Z_1 + Z_2 = 1$) are very simple functions of the density which can be found in Ref. [9]. As explained in detail in this last reference, the pion strength function splits into two collective eigenmodes. Of special interest is the lower branch (Ω_1), sometimes called the pionic branch responsible for the softening of the pion dispersion curve. To calculate the medium modified π - π T matrix, we have to solve the LS equation [Eq. (18)] with a modified two-pion propagator according to

$$G_{2\pi}(\mathbf{k}, E) = \int \frac{idk_0}{2\pi} D_\pi(\mathbf{k}, k_0) D_\pi(-\mathbf{k}, E - k_0). \quad (24)$$

In the two-level model, its explicit expression is

$$G_{2\pi}(\mathbf{k}, E) = \sum_{i,j=1}^2 \frac{\Omega_i(k) + \Omega_j(k)}{2\Omega_i(k)\Omega_j(k)} \times \frac{Z_i(k)Z_j(k)}{E^2 - (\Omega_i(k) + \Omega_j(k))^2 + i\eta}. \quad (25)$$

Obviously, in the absence of p -wave coupling, one recovers Eq. (19). In a more realistic description the main features of the two-level model survive but the modes $\Omega_{1,2}$ acquire a

width. This can be incorporated through the replacement in the pion propagator [Eq. (23)]:

$$\Omega_j(k) \rightarrow \Omega_j(k) + i \frac{\text{Im} \tilde{\Pi}^0(\mathbf{k}, \Omega_j(k))}{2\Omega_j(k)}, \quad (26)$$

where $\text{Im} \tilde{\Pi}^0$, calculated along the line j , takes into account the delta width, corrected from Pauli blocking, together with extra two-particle-two-hole (2p-2h) contributions which are not reducible to a delta width piece. Details are given in Ref. [24]. The imaginary part of the two-pion propagator is obtained through a spectral representation

$$\text{Im} G_{2\pi}(\mathbf{k}, E) = -\frac{1}{\pi} \int_0^E d\omega \text{Im} D_\pi(\mathbf{k}, E) \text{Im} D_\pi(\mathbf{k}, E - \omega). \quad (27)$$

The real part is calculated with a dispersion relation.

V. RESULTS

To clearly illustrate the basic physical mechanisms, we present the results for the in medium pion-pion scattering matrix in the simplified calculational scheme discussed in the previous sections, using systematically the second set of parameters with $m_\sigma = 1$ GeV. First, the treatment of collective $\pi N\Delta$ configurations entering the two-pion propagator is done in the extended two-level model summarized just above. In addition we use the leading order term of the so-called $1/N$ expansion of the linear sigma model. In a forthcoming paper we will incorporate the full linear sigma model potential together with a full calculation of the in-medium two-pion propagator. However, we believe that the conclusions concerning the relative weight of collective pionic modes and chiral symmetry restoration will remain valid. The linear sigma model can be seen as a $O(N+1)$ model with $N=3$. It has been shown [25,15] that, to leading order in a $1/N$ expansion, one gets a consistent symmetry conserving approach fulfilling Ward identities and all chiral symmetry constraints. The corresponding potential is obtained from Eq. (16) by simply keeping the s channel pole term and dropping the u and t sigma propagators. In practice it has the great advantage of making the potential separable. According to [15], we take the potential as

$$\langle \mathbf{k}, -\mathbf{k} | V(E) | \mathbf{k}', -\mathbf{k}' \rangle = 6v(k)v(k')\lambda \frac{E^2 - m_\pi^2}{E^2 - m_\sigma^2} \quad \text{with}$$

$$\lambda = \frac{m_\sigma^2 - m_\pi^2}{2f_\pi^2}, \quad (28)$$

with a phenomenological form factor $v(k) = g/(1 + k^2/q_d^2)^\alpha$. It is important to note that the introduction of such a form factor does not destroy in any way the chiral symmetry properties. Taking $g=0.9$, $\alpha=3$, and $q_d=1$ GeV one gets a reasonable fit to experimental phase shifts [15]. With such a separable potential one easily obtains the explicit form of the T matrix:

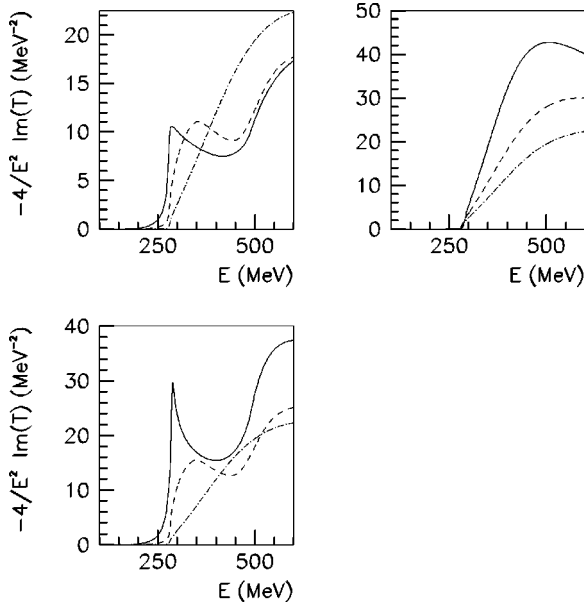


FIG. 6. Strength function for the π - π interaction at zero density (dot-dashed curves), half nuclear matter density (dashed curves), and normal nuclear matter density (solid curves). (a) (upper left panel) corresponds to a calculation with coupling to the pionic collective modes, keeping m_σ , m_π , and f_π at their vacuum values. (b) (upper right panel) incorporates the in-medium modification of m_σ , m_π , and f_π from the NJL model, ignoring the effect of collective pionic modes. (c) (lower panel) incorporates both effects. We use the parameter set II with $m_\sigma=1$ GeV.

$$\langle \mathbf{k}, -\mathbf{k} | T(E) | \mathbf{k}', -\mathbf{k}' \rangle = 6v(k)v(k')\lambda \times \frac{E^2 - m_\pi^2}{E^2 - m_\sigma^2 - 3\lambda(E^2 - m_\pi^2)\Sigma(E)}, \quad (29)$$

with $\Sigma(E)$ given by

$$\Sigma(E) = \int \frac{d^3q}{(2\pi)^3} v^2(q) G_{2\pi}(\mathbf{q}, E). \quad (30)$$

In Fig. 6, we present the results of the calculation for the π - π strength function (i.e., the imaginary part of the scattering amplitude) for zero density, half nuclear matter density ($0.5\rho_0$), and normal nuclear matter density (ρ_0). We limit ourselves to the low-energy sector ($E < 600$ MeV) since it corresponds to the domain of validity of the low energy effective theory and to the region experimentally probed for instance in the CHAOS experiment. In Fig. 6(a) we keep the sigma mass, the pion mass, and the pion decay constant at their vacuum values and incorporate the effects of p -wave $\pi N\Delta$ collective modes. We recover the well-known structure near the two-pion threshold originating from the softening of the pion dispersion relation and extensively discussed in [1,9,10]. In Fig. 6(b), we disregard the effect of these pionic modes but simply replace in the vacuum T matrix the sigma mass, the pion mass, and the pion decay constant by their in-medium value. In this way we isolate the effects intimately related to chiral symmetry restoration. We see a

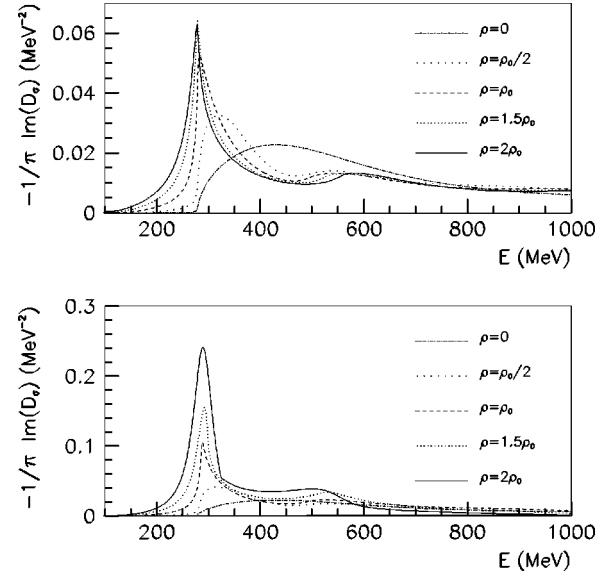


FIG. 7. Spectral function for the sigma meson at various densities. (a) (upper panel) corresponds to a calculation with coupling to the pionic collective modes, keeping m_σ , m_π , and f_π at their vacuum values. (b) (lower panel) incorporates the in-medium modification of m_σ , m_π , and f_π from the NJL model on top of collective pionic modes. We use the parameter set II with $m_\sigma=1$ GeV.

spectacular enhancement of the strength with increasing density which is roughly uniform in the energy domain considered. The origin of this effect is mainly the dropping of the sigma mass. However, it is less pronounced in the density domain typical of ordinary nuclei than in the work of Hatsuda *et al.* [20] for at least two obvious reasons. First, we start with a vacuum sigma mass of 1 GeV (used in our previous works to fit the phase shifts) significantly larger than the values of 550 MeV or 750 MeV used in [20]. Second, the $\sigma\pi\pi$ coupling constant $\lambda = m_\sigma^2 - m_\pi^2 / 2f_\pi^2$ slightly decreases at variance with the work of Hatsuda *et al.* where it was density independent. We will come to a more detailed comparison of the two works when discussing the sigma propagator itself. In Fig. 6(c), we include simultaneously the two mechanisms. We recover the typical low energy structure associated with pionic collective modes but significantly reinforced by the effect of chiral symmetry restoration.

To study the evolution with density of scalar-isoscalar modes, it is also very interesting to study the sigma meson spectral function, i.e., the imaginary part of the sigma propagator. It is a simple matter to obtain the explicit form of the sigma meson propagator in this simple model [15]:

$$D_\sigma(E) = \frac{1}{E^2 - m_\sigma^2 - S_\sigma(E)}, \quad (31)$$

with the sigma self-energy given by

$$S_\sigma(E) = \frac{6f_\pi^2\lambda^2\Sigma(E)}{1 - 3\lambda\Sigma(E)}. \quad (32)$$

The results of the calculation are shown in Fig. 7 for the three previous cases: pionic collective modes only [Fig.

6(a)], chiral symmetry restoration only [Fig. 6(b)], and both [Fig. 6(c)]. It is also interesting to compare our results with the calculation of Ref. [18] where chiral symmetry restoration is implemented by only dropping the sigma mass, ignoring the modification of the $\sigma\pi\pi$ coupling constant. Since we find in this present work that λ is only slightly modified (about 20% lower at $\rho=\rho_0$), it is not surprising that the reinforcement of the low energy enhancement is qualitatively similar in these two works, at least at normal nuclear matter density.

Until now we have considered the density regime accessible in experiments on ordinary nuclei such as the CHAOS experiments. It is, however, extremely interesting to go beyond, although the basics nuclear physics ingredients of the calculation are less under control. We now follow for a while the arguments of [20]. Let us consider the spectral function of the sigma meson:

$$\begin{aligned}\rho_\sigma(E) &= -\frac{1}{\pi}\text{Im}D_\sigma(E) \\ &= -\frac{1}{\pi}\frac{\text{Im}S_\sigma(E)}{[E^2-m_\sigma^2-\text{Re}S_\sigma(E)]^2+[\text{Im}S_\sigma(E)]^2},\end{aligned}\quad (33)$$

where m_σ is as usual the in-medium sigma meson mass obtained here from the NJL model. As in the work of Hatsuda *et al.* [20], this in-medium sigma meson mass has an evolution which follows linearly at low density the scalar condensate. However, the precise law of evolution is different since it comes from a nucleonic tadpole diagram in [20]. Near the two-pion threshold the phase space factor yields to the well-known behavior:

$$\text{Im}D_\sigma \sim \text{Im}S_\sigma \sim (E^2 - 4m_\pi^2)^{1/2}. \quad (34)$$

Before chiral symmetry restoration with complete $\sigma-\pi$ degeneracy, there must exist a density at which $\text{Re}D_\sigma^{-1}(E=2m_\pi)=0$ or $4m_\pi^2 - m_\sigma^2 - S(E=2m_\pi)=0$. At such a density ρ_d , ignoring the effect of pionic collective modes, the spectral function behaves as

$$\begin{aligned}\rho_\sigma(E \simeq 2m_\pi) &= -\frac{1}{\pi}\frac{1}{\text{Im}S_\sigma(E \simeq 2m_\pi)} \\ &\sim \theta(E - 2m_\pi)/(E^2 - 4m_\pi^2)^{1/2}.\end{aligned}\quad (35)$$

This implies that there arises a mild integrable singularity just above the two-pion threshold in the medium. With our set of parameters this precursor effect of chiral symmetry restoration occurs at a density slightly larger than $2\rho_0$ at variance with [20] where this density was found at $1.25\rho_0$. In addition when collective pionic modes are included, there is strength below two-pion threshold due to the various sources of width ($\Delta-h$, $2p-2h$). As a consequence, the mathematical singularity disappears. However, a precursor effect still manifests itself through a strong enhancement of the near-threshold structure created by the p -wave pionic collective modes. This feature is illustrated in Fig. 7 where the influ-

ence of chiral symmetry restoration itself is visible by comparison of Fig. 7(a) and Fig. 7(b).

VI. CONCLUSION

In this paper we have examined medium effects on the unitarized pion-pion interaction in the scalar-isoscalar channel and the sigma-meson spectral function. The new feature of this work is the simultaneous treatment of chiral symmetry restoration and the nuclear effect associated with the existence of collective pionic modes. Starting from the standard Nambu–Jona-Lasinio model generalized at finite density, we have obtained an in-medium pion-pion potential. In particular, we have shown that the NJL model regenerates the linear sigma model potential but with modified parameters (m_σ , m_π , and f_π). This modification of the parameters intimately related to chiral symmetry restoration strongly reinforces the $\pi\pi$ strength function in the threshold region. Since the NJL model is not adapted to the calculation of collective pionic modes, we have used the standard phenomenological nuclear physics approach. When both effects are incorporated, the low-energy $\pi\pi$ structure resulting from the existence of nuclear collective modes is significantly enhanced, in particular through the dropping of the sigma mass. This feature is obviously of considerable importance for the understanding of the structure observed by the CHAOS Collaboration in $\pi-2\pi$ experiments on various nuclei.

ACKNOWLEDGMENTS

We are indebted to Z. Aouissat, J. Delorme, M. Ericson, J. Marteau, P. Schuck, and J. Wambach for stimulating and enlightening discussions.

APPENDIX

We list below the various integrals appearing in the text:

$$I(p) = \int \frac{d^4k}{(2\pi)^4} \frac{1}{[k^2 - m^2][(k+p)^2 - m^2]}, \quad (A1)$$

$$K(p) = \int \frac{d^4k}{(2\pi)^4} \frac{1}{[k^2 - m^2]^2[(k+p)^2 - m^2]}, \quad (A2)$$

$$L(p) = \int \frac{d^4k}{(2\pi)^4} \frac{1}{[k^2 - m^2]^2[(k+p)^2 - m^2]^2}, \quad (A3)$$

$$I_{mn}(p) = \int \frac{d^4k}{(2\pi)^4} \frac{1}{[k^2 - m^2]^m[(k+p)^2 - m^2]^n}. \quad (A4)$$

The above equations are strictly valid at $T=0$. The explicit expressions at finite temperature are given in [19] and

can be straightforwardly extended at both finite density and temperature. Here we simply quote a few relevant results for numerical calculation at finite density:

$$-iI(p_0) = \int_{k_F}^{\Lambda} \frac{dk}{2\pi^2} \frac{k^2}{E} \frac{-1}{p_0^2 - 4E^2},$$

$$-iK(p_0) = \int_{k_F}^{\Lambda} \frac{dk}{2\pi^2} \frac{-k^2}{4E^3} \left[\frac{1}{p_0^2 - 4E^2} - \frac{8E^2}{(p_0^2 - 4E^2)^2} \right],$$

$$-iL(p_0) = \int_{k_F}^{\Lambda} \frac{dk}{4\pi^2} \frac{k^2}{4E^3 p_0^2} \left[\frac{1}{p_0^2 - 4E^2} - \frac{12E^2}{(p_0^2 - 4E^2)^2} - \frac{64E^4}{(p_0^2 - 4E^2)^3} \right], \quad (\text{A5})$$

and the gap equation is

$$M = m + 4N_c N_f g \int_{k_F}^{\Lambda} \frac{k^2 dk}{2\pi^2} \frac{M}{E}. \quad (\text{A6})$$

-
- [1] P. Schuck, W. Nörenberg, and G. Chanfray, *Z. Phys. A* **330**, 119 (1988).
- [2] P. Guichon and J. Delorme, *Phys. Lett. B* **263**, 157 (1991).
- [3] T. Udagawa, S. W. Hong, and F. Osterfeld, *Phys. Lett. B* **245**, 1 (1990).
- [4] D. Contardo *et al.*, *Phys. Lett.* **168B**, 331 (1986).
- [5] T. Hennino *et al.*, *Phys. Lett. B* **283**, 42 (1992); **303**, 236 (1993).
- [6] H. Esbensen and T. S. H. Lee, *Phys. Rev. C* **32**, 1966 (1985).
- [7] E. Oset, E. Shiino, and H. Toki, *Phys. Lett. B* **224**, 249 (1989).
- [8] P. Fernandez de Cordoba, E. Oset, and M. J. Vicente-Vacas, *Nucl. Phys.* **A592**, 472 (1995).
- [9] G. Chanfray, Z. Aouissat, P. Schuck, and W. Nörenberg, *Phys. Lett. B* **256**, 325 (1991).
- [10] Z. Aouissat, R. Rapp, G. Chanfray, P. Schuck, and J. Wambach, *Nucl. Phys.* **A581**, 471 (1995).
- [11] J. W. Durso, H. C. Kim, and J. Wambach, *Phys. Lett. B* **298**, 267 (1993).
- [12] R. Rapp, J. W. Durso, and J. Wambach, *Nucl. Phys.* **A615**, 501 (1997).
- [13] R. Rapp, R. Machleidt, J. W. Durso, and G. E. Brown, *Phys. Rev. Lett.* **82**, 1827 (1999).
- [14] F. Bonutti *et al.*, CHAOS Collaboration, *Phys. Rev. Lett.* **77**, 603 (1996).
- [15] P. Schuck *et al.*, nucl-th/9806069.
- [16] R. Rapp *et al.*, *Phys. Rev. C* **59**, R1237 (1999).
- [17] M. J. Vicente Vacas and E. Oset, *Phys. Rev. C* **60**, 064621 (1999).
- [18] Z. Aouissat, G. Chanfray, P. Schuck, and J. Wambach, nucl-th/9908076.
- [19] E. Quack, P. Zhuang, Y. Kalinovsky, S. P. Klevansky, and J. Hüfner, *Phys. Lett. B* **348**, 1 (1995).
- [20] T. Hatsuda, T. Kunihiro, and H. Shimizu, *Phys. Rev. Lett.* **82**, 2840 (1999); T. Hatsuda and T. Kunihiro, nucl-th/9901020; nucl-th/9902025.
- [21] Y. Nambu and G. Jona-Lasinio, *Phys. Rev.* **122**, 345 (1961); **124**, 246 (1961).
- [22] T. Hatsuda and T. Kunihiro, *Suppl. Prog. Theor. Phys.* **91**, 284 (1987).
- [23] H. J. Schulze, *J. Phys. G* **21**, 185 (1995).
- [24] G. Chanfray and P. Schuck, *Nucl. Phys.* **A555**, 329 (1993).
- [25] Z. Aouissat, P. Schuck, and J. Wambach, *Nucl. Phys.* **A618**, 402 (1997).